

The Equation of State of Nuclear Matter, and Nuclei in Laboratories and in Neutron-Star Crusts

K. Oyamatsu¹ and K. Iida²

¹*Department of Media Theories and Production, Aichi Shukutoku University
Nagakute, Nagakute-cho, Aichi-gun, Aichi 480-1197, Japan*

²*RIKEN BNL Reseach Center, Brookhaven National Laboratory
Upton, New York 11973-5000, U.S.A.*

email: oyak@asu.aasa.ac.jp

Abstract

We examine a relationship between the phenomenological equation of state (EOS) of nuclear matter near normal nuclear density and neutron-rich nuclei in laboratories and in neutron-star crusts. In this study, we use about 200 EOS's, which are systematically constructed in such a way as to provide a reasonable fit to empirical masses and radii of stable nuclei by simplified Thomas-Fermi calculations. As for neutron-rich nuclei in laboratories, matter radii and masses are shown to be functions of the symmetry energy density derivative coefficient L . We also find that the boundary density between the core and crust of neutron stars is a decreasing function of L . We expect that future systematic measurements of the matter radii and masses of neutron-rich nuclei could help deduce the L value, which in turn could give useful information about nuclei in neutron-star crusts.

1 Introduction

The equation of state (EOS) of nuclear matter plays a key role in determining macroscopic nuclear properties of nuclei in laboratories and in neutron-star crusts. The saturation density and energy of symmetric nuclear matter, which consists of an equal number of neutrons and protons, are determined fairly well from masses and radii of stable nuclei, in which neutrons and protons are not very different in number. In the near future, a radioactive ion beam will enable us to measure nuclear masses and radii of heavy unstable nuclei with large neutron excess. This could open a door to explore extremely neutron-rich nuclei in neutron-star crusts. In order to make full use of the future experiment for the purpose of deducing asymmetric matter EOS, it is important to clarify what kind of EOS properties can be determined from stable nuclei, and what kind of EOS properties can not be determined from stable nuclei but from neutron-rich unstable nuclei. In this paper, we focus on the empirical saturation properties of the EOS that can be deduced from stable nuclei.

The energy per nucleon near the saturation point of symmetric nuclear matter is generally expressed as

$$w = w_0 + \frac{K_0}{18n_0^2}(n - n_0)^2 + \left[S_0 + \frac{L}{3n_0}(n - n_0) \right] \alpha^2. \quad (1)$$

Here w_0 , n_0 and K_0 are the saturation energy, the saturation density and the incompressibility of symmetric nuclear matter. The neutron excess is defined as $\alpha = 1 - 2x$ using proton fraction x .

The parameters S_0 (the symmetry energy) and L (the density symmetry coefficient) characterize the density dependent symmetry energy $S(n)$ at $n \approx n_0$ as;

$$S_0 = S(n_0), \quad (2)$$

$$L = 3n_0(dS/dn)_{n=n_0}, \quad (3)$$

From Eq. (1), the saturation density n_s and energy w_s of asymmetric nuclear matter with fixed proton fraction are given, up to the second order of α , by

$$n_s = n_0 - \frac{3n_0L}{K_0}\alpha^2, \quad (4)$$

$$w_s = w_0 + S_0\alpha^2. \quad (5)$$

2 Macroscopic description of nuclei

In constructing a macroscopic nuclear model, we begin with a simple expression for the bulk energy per nucleon [1, 4],

$$w = \frac{3\hbar^2(3\pi^2)^{2/3}}{10m_n n} (n_n^{5/3} + n_p^{5/3}) + (1 - \alpha^2)v_s(n)/n + \alpha^2 v_n(n)/n, \quad (6)$$

where

$$v_s = a_1 n^2 + \frac{a_2 n^3}{1 + a_3 n} \quad (7)$$

and

$$v_n = b_1 n^2 + \frac{b_2 n^3}{1 + b_3 n} \quad (8)$$

are the potential energy densities for symmetric nuclear matter and pure neutron matter, and m_n is the neutron mass. Here, replacement of the proton mass m_p by m_n in the proton kinetic energy makes only a negligible difference. Equation (6) can well reproduce the microscopic calculations of symmetric nuclear matter and pure neutron matter by Friedman and Pandharipande [2] and of asymmetric nuclear matter by Lagaris and Pandharipande [3]. Furthermore the expression can also reproduce phenomenological Skyrme Hartree-Fock and relativistic mean field EOS's.

The values of the parameters included in Eqs. (7) and (8) will be chosen below in such a way that they reproduce data on radii and masses of *stable* nuclei. In the limit of $n \rightarrow n_0$ and $\alpha \rightarrow 0$ ($x \rightarrow 1/2$), expression (6) reduces to the usual form (1) [4].

We describe a spherical nucleus of proton number Z and mass number A within the framework of a simplified version of the extended Thomas-Fermi theory [1]. We first write the total energy of a nucleus as a function of the density distributions $n_n(\mathbf{r})$ and $n_p(\mathbf{r})$ according to

$$E = \int d^3r n(\mathbf{r})w(n_n(\mathbf{r}), n_p(\mathbf{r})) + F_0 \int d^3r |\nabla n(\mathbf{r})|^2 + \frac{e^2}{2} \int d^3r \int d^3r' \frac{n_p(\mathbf{r})n_p(\mathbf{r}')}{|\mathbf{r} - \mathbf{r}'|} + Nm_n + Zm_p, \quad (9)$$

where the first, second and third terms on the right hand side are the bulk energy, the gradient energy with an adjustable constant F_0 , and the Coulomb energy, respectively. The symbol $N = A - Z$ denotes the neutron number. Here we ignore shell and pairing effects. We also neglect the contribution to the gradient energy from $|\nabla(n_n(\mathbf{r}) - n_p(\mathbf{r}))|^2$; this contribution makes only a little difference even in the description of extremely neutron-rich nuclei, as clarified in the context of neutron star matter [1].

For the present purpose of examining the macroscopic properties of nuclei such as masses and radii, it is sufficient to characterize the neutron and proton distributions for each nucleus by the central densities, radii and surface diffuseness different between neutrons and protons, as in Ref. [1]. We thus assume the nucleon distributions $n_i(r)$ ($i = n, p$), where r is the distance from the center of the nucleus, as

$$n_i(r) = \begin{cases} n_i^{\text{in}} \left[1 - \left(\frac{r}{R_i} \right)^{t_i} \right]^3, & r < R_i, \\ 0, & r \geq R_i. \end{cases} \quad (10)$$

Here R_i roughly represents the nucleon radius, t_i the relative surface diffuseness, and n_i^{in} the central number density. The proton distribution of the form (10) can fairly well reproduce the experimental data for stable nuclei such as ^{90}Zr and ^{208}Pb [1].

About 200 sets of the EOS parameters a_1 – b_2 and F_0 are determined in Refs. [4] from masses and radii of stable nuclei using the empirical values for nine nuclei on the smoothed β -stability line ranging $25 \leq A \leq 245$. All of the EOS's reproduce the input nuclear data almost equally. Although we fixed the b_3 value (1.58632 fm^3) in such a way as to reproduce pure neutron matter EOS by Friedman and Pandharipande [2], this artificial constraint on b_3 was found to make little difference in determining the the other EOS parameters [7].

As shown in Fig. 1, there is a strong empirical correlation between S_0 and L [4],

$$S_0 \approx B + CL, \quad (11)$$

with $B \approx 28 \text{ MeV}$ and $C \approx 0.075$. It is noteworthy that a similar result, $B = 29 \text{ MeV}$ and $C = 0.1$, was obtained from various Hartree-Fock models with finite-range forces by Farine et al. [5]. This correlation is the only information for asymmetric nuclear matter that can be obtained from stable nuclei. This is the reason why there is significant difference in the behavior at large neutron excess among the models for asymmetric matter EOS although they reproduce the properties of stable nuclei.

As for the saturation energy and density of symmetric nuclear matter, $w_0 = -16.1 \pm 0.2$ and $n_0 \approx 0.16$ while there is a weak correlation between n_0 and K_0 [4]. This is a feature found among non-relativistic phenomenological Skyrme Hartree-Fock EOS's (see Fig. 4 of Ref. [6]).

In Fig. 2, the uncertainties in L and K_0 are represented as a band. The upper bound reaches a large value of L , which increases with increase in K_0 .

Hence it is interesting to examine how these uncertainties in L and K_0 reflect nuclear structure calculations of neutron-rich nuclei in laboratories and in neutron stars.

3 Neutron-rich nuclei in laboratories

Using the nearly 200 EOS's, we calculate masses and radii of extremely neutron-rich heavy nuclei, which could be produced in laboratories in the future. For example, Figures 3 and 4 show the root-mean-square matter radius and mass excess of ^{80}Ni ($N = 52, Z = 28, Z/A \approx 0.35$). We see clearly that the matter radius and mass of extremely neutron-rich nuclei are dependent on L . This reflects the fact that the saturation density and energy, which naively communicate with the radius and mass, are approximately linear functions of L (see Eqs. (4), (5), (11)) [4, 8].

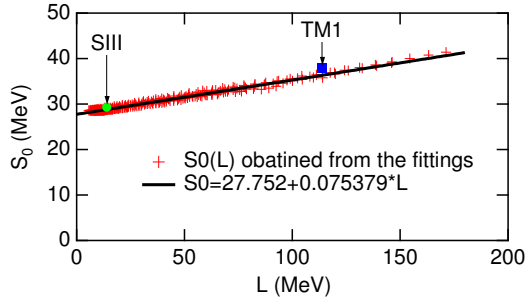


Figure 1: The correlation between S_0 and L deduced from the mass and radius data for stable nuclei.

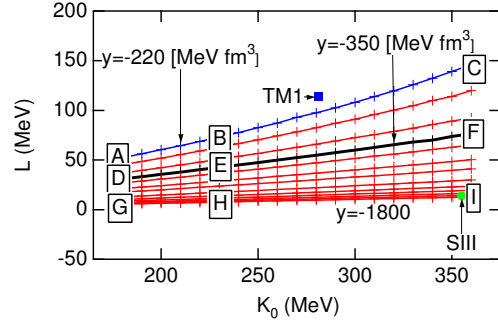


Figure 2: The (L, K_0) values consistent with the mass and radius data for stable nuclei.

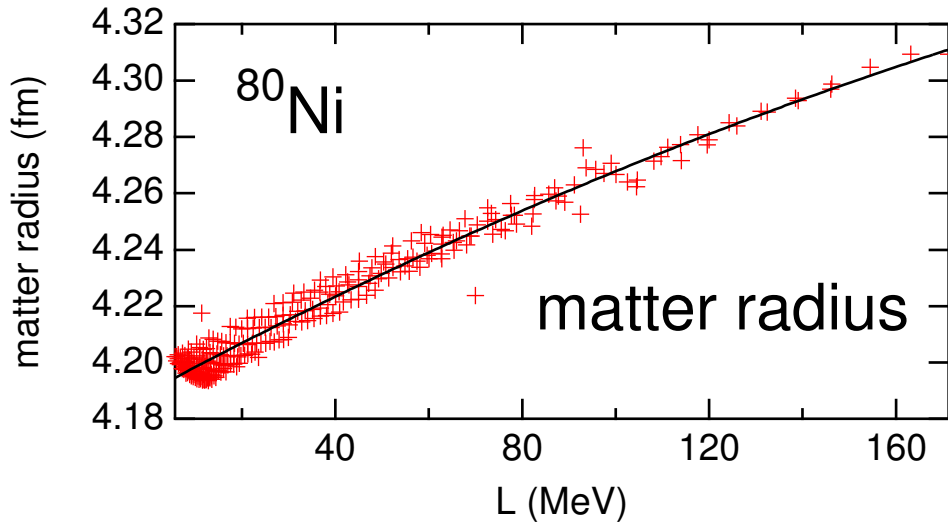


Figure 3: The calculated matter radius of ^{80}Ni .

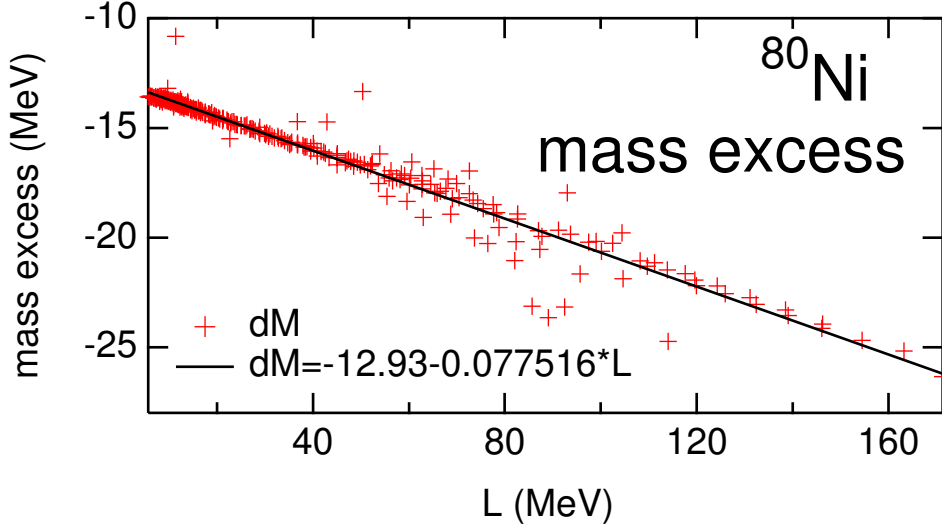


Figure 4: The calculated mass excess of ^{80}Ni .

4 Inner boundary of a neutron star crust

It is also interesting to explore extremely neutron-rich nuclei in neutron-star crust, where nuclei are embedded in a gas of dripped neutrons and the nuclei may take exotic pastalike shapes. Among various interesting properties, we calculate the boundary density between the crust and the core, at which the nuclei melt into uniform matter. Here, we examine how the uncertainties of the EOS reflect the determination of the boundary density. Figure 5 shows the approximate boundary density obtained from the nearly 200 EOS's. In this calculation we follow a line of argument of Pethick et al. [9]. From Fig. 5, we see clearly that the boundary density is a decreasing function of L . This behavior may be understood from the fact that L acts to make shallow the single particle potential depth of bound protons in nuclei in neutron-star crusts.

5 Summary

We examine the macroscopic properties of neutron-rich nuclei in laboratories and in neutron-star crusts using about 200 sets of the EOS parameters that are systematically obtained from fitting to masses and radii of stable nuclei. In the series of our studies, we adopt a simplified Thomas-Fermi model allowing for large uncertainties in the K_0 and L values.

As for the relationship between the EOS parameters, the saturation density n_0 has a weak K_0 dependence while the saturation energy w_0 is essentially constant. There is a strong correlation between S_0 and L : $S_0 = 28 + 0.075L$ (MeV). However, the L value can not be constrained from stable nuclei although the upper bound of L can be estimated as an increasing function of K_0 . Since there remains uncertainties in L and K_0 , our EOS models vary significantly at large neutron excess, even though they reproduce the properties of stable nuclei almost equally.

Using the EOS's obtained for various sets of the L and K_0 values, we systematically examine the macroscopic properties of extremely neutron-rich nuclei in laboratories and in neutron stars. As for laboratory nuclei, the predicted matter radii and masses are dependent on L . This L

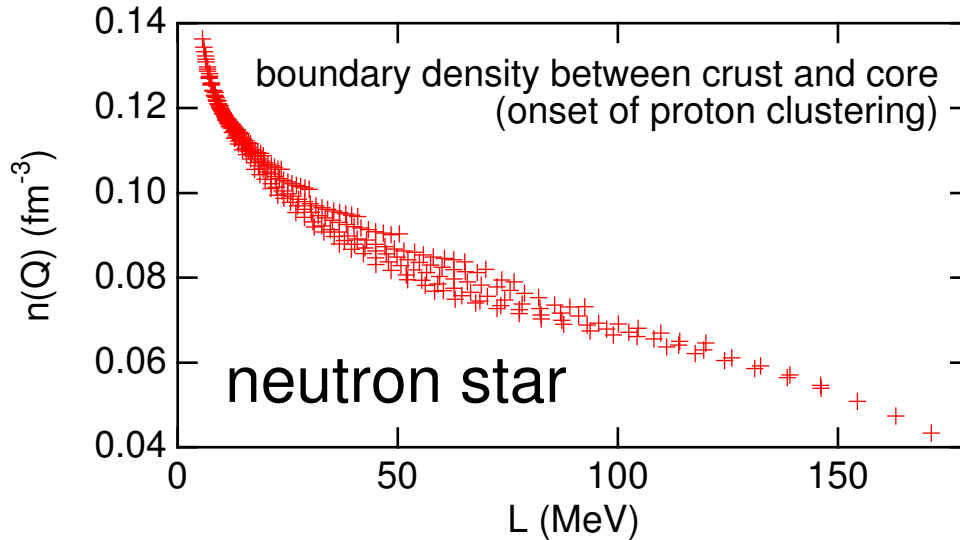


Figure 5: The crust-core boundary density in a neutron star.

dependence comes from the fact that the saturation energy and density of asymmetric matter are almost linear functions of L . As for nuclei in neutron-star crusts, we examine the crust-core boundary density, where nuclei melt into uniform matter. It is found that the density is a decreasing function of L . This is relevant to the fact that L controls the proton potential depth in nuclei.

From these results, we conclude that future systematic measurements of the matter radii and masses of neutron-rich nuclei could help deduce the L value, which in turn could give useful information about nuclei in neutron star crusts.

References

- [1] K. Oyamatsu, Nucl. Phys. A 561 (1993) 431.
- [2] B. Friedman, V.R. Pandharipande, Nucl. Phys. A 361 (1981) 502.
- [3] I.E. Lagaris, V.R. Pandharipande, Nucl. Phys. A 369 (1981) 470.
- [4] K. Oyamatsu, K. Iida, Prog. Theor. Phys. 109 (2003) 631.
- [5] M. Farine, J.M. Pearson, B. Rouben, Nucl. Phys. A 304 (1978) 317.
- [6] J.P. Blaizot, Phys. Rep. **64**, 171 (1980).
- [7] K. Oyamatsu, K. Iida, Proc. 2003 Symposium on Nuclear Data, JAERI-Conf 2004-005, (2004), 184.
- [8] K. Oyamatsu, I. Tanihata, Y. Sugahara, K. Sumiyoshi, H. Toki, Nucl. Phys. A 634 (1998) 3.
- [9] C.J. Pethick, D.G. Ravenhall, C.P. Lorenz, Nucl. Phys. A 584 (1995) 675.